2018 European Control Conference (ECC)
June 12-15, 2018. Limassol, Cyprus

On the design of an observer for the detection of null-current shifts in an electro-hydraulic actuation system*

Tomas Puller†, Andrea Lecchini-Visintini†, Matthew C. Turner†

***Abstract*— This paper presents a nonlinear observer for estimating the null current in an electro-hydraulic actuation system. The actuation system's model consists of the interconnection of a linear system, with two poles on the imaginary axis, and a static nonlinearity, with characteristics similar to a time-varying deadzone. This combination of features means that many standard observer techniques cannot be proven to provide a good estimate of the null current. It is, however, shown that a partitioning of the nonlinearity, together with a nonlinear observer constructed using inspiration from the literature, enables one to conclude global uniform ultimate boundedness of the observation error. Moreover, the size of the region of ultimate boundedness depends, naturally, on the parameters of the deadzone-like nonlinearity. Simulations on a high-fidelity simulation involving the hydraulic actuator show the effectiveness of the proposed observer.**

I. INTRODUCTION

In this work we consider an electro-hydraulic actuation system employed in the variable geometry control of a jet engine compressor. A schematic representation of the actuation system is provided in Fig. 1. The control input is Torque Motor Current (TMC) and the controlled output is the position of the piston in the hydraulic cylinder X_{VSVA} (Variable Stator Vanes Actuator). The other variables included in the picture are pressures which are determined by the flight conditions. The control input TMC can assume positive and negative values. The positive value TMC_0 corresponds to a null piston velocity. Values larger, or smaller, than TMC_0 correspond respectively to a positive (extension), or negative (retraction), velocity of the piston. The choice of a positive null-current level is standard industrial practice, see e.g. the 4-20 mA current loop [3]. In addition to adhering to standard practice, in this particular case a positive TMC_0 implements the specific safety requirement of enforcing a slow retraction in the case of a power loss. The dynamics of the actuation system are characterised by the presence of a 'deadzone' input nonlinearity. Deadzone nonlinearities are a common occurrence in the models of hydraulic actuators, but usually account for valve overlaps (see e.g. [4], [5], [6]). However, in this case, the deadzone is caused by the presence of a cooling flow established through an orifice in the piston. The reader is referred to [1], and to the preliminary contribution [2], for a detailed introduction to the system and the development of a simplified model of the actuation system. The simplified model is recalled in Section II.

*This work was supported by Rolls-Royce Control Systems, UK

† T.P., A.L.V. and M.C.T. are with the Computational Engineering and Control Group, Department of Engineering, University of Leicester, UK. Email: {tp139, alv1, mct6}@leicester.ac.uk

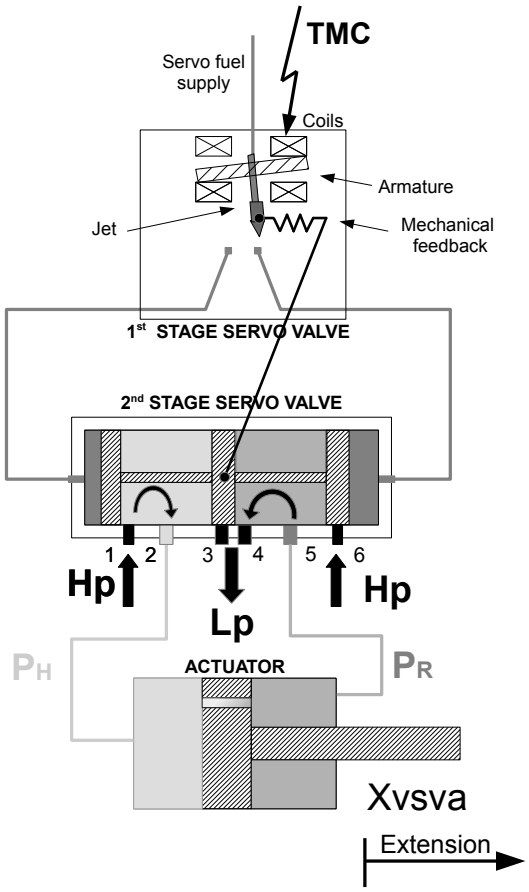

Fig. 1. Scheme of the electro-hydraulic actuation system[1].

In this work we focus on the problem of detecting shifts in the value of the null-current TMC_0, which can happen in case of an electrical fault (e.g. turn-to-turn coil short circuit). The problem is interesting because, as will be seen shortly, it contains a combination of features which make the application of standard observer theory difficult. In control theoretic terms, the plant itself can be approximated by the cascade of a deadzone-like nonlinearity and an integrator, with the inputs being the (known) control signal and an unknown but constant input. This produces a double integrator system containing a troublesome nonlinearity. Although it can be proved that the deadzone nonlinearity is slope-restricted, because the plant is not open-loop stable and because the deadzone lacks gain at the origin, it is not possible to invoke "standard" absolute stability (see [14], [17], [16], [15]) results in order

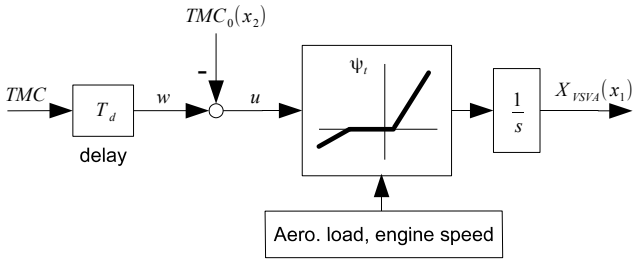

Fig. 2. Simplified model of the actuation system

to guarantee stability of the observation error. Similarly, because some parameters of the nonlinearity are not precisely known, and also known to vary, the system does not fit into typical nonlinear observer design frameworks. For example, most nonlinear observers incorporate a *duplication* of the nonlinearity in their dynamics (see, for example, Chapter 11 of [18]) so a reasonably good estimate of the nonlinearity needs to be available. The problem under consideration is most closely related to the Circle-Criterion inspired observer designs [7], [8] and so we propose modifications to these approaches in order to obtain a suitable nonlinear observer design algorithm.

The actuation system considered in this work is a sub-assembly of the Hydro-Mechanical Unit (HMU) of the Rolls-Royce Trent 1000 turbofan engine and is manufactured by Rolls-Royce Control Systems (RRCS) in Birmingham, UK. The performance of the observer developed in this work is illustrated in simulations using the Trent 1000 Real System Simulator (RSS). The simulations generated by the Trent 1000 RSS are considered to be very accurate and are employed by RRCS as surrogate experimental data for development and certification purposes.

The paper is structured as follows. The next section describes the characteristics of the actuation system model considered in this paper and the following section describes the construction of a nonlinear observer which can guarantee global ultimate boundedness of the observation error. After this, simulations on the RSS are presented; the paper closes with some concluding remarks. Appendix A contains a technical remark on the motivation for this work. Appendix B contains proofs.

The following notation is adopted: if e is a vector valued signal then $\|e\|$ is the point-wise 2-norm, if $\mathbf{A}$ is a matrix then $\|\mathbf{A}\|$ is the corresponding induced matrix norm, i.e. maximum singular value.

II. Model of the actuation system

The simplified actuation system's model is depicted in Fig. 2. It includes a pure delay, which represents the dynamics of the first stage servovalve (see Fig. 1), and a static, but possibly time-varying, relation between the control input and the velocity of the piston in the hydraulic cylinder. The time-varying features of the input nonlinearity depend on external variables (engine speed and aerodynamic load). The following notation is adopted: w is the delayed control input (i.e. delayed TMC), x_1 is the position of the actuator's piston, x_2 is the value of the null current (i.e. TMC_0), and $u = w - x_2$. In view of developing an observer for the detection of null-current shifts, x_2 is assumed to be a constant state. This is consistent with assuming that TMC_0 is constant but subject to step-like shifts. Note that, in principle, since TMC_0 is a feature of the first stage servovalve also x_2 should be a delayed version of TMC_0. However, since TMC_0 is assumed to be a constant this is immaterial.

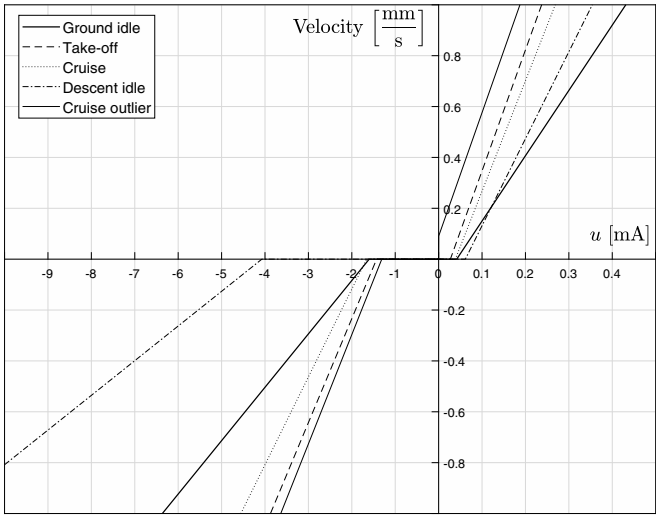

Fig. 3. Instances of ψ_t for selected flight conditions. Note the different scalings for positive and negative values of u.

The equations of the model are:

$$\dot{x}_1 = \psi_t(w - x_2) \tag{1}$$

$$\dot{x}_2 = 0 \tag{2}$$

where the static input nonlinearity ψ_t can be written as

$$\psi_t(u) = \begin{cases} (M_t^E/2)\left[1 + \text{sgn}(u - \bar{u}_t^E)\right]\left(u - \bar{u}_t^E\right), & u \geq 0 \\ \\ (M_t^R/2)\left[1 - \text{sgn}(u - \bar{u}_t^R)\right]\left(u - \bar{u}_t^R\right), & u < 0. \end{cases} \tag{3}$$

with time-varying coefficients M_t^E, M_t^R, $\bar{u}_t^E$ and $\bar{u}_t^R$ which depend on the external variables. The superscripts E and R discriminate between extension ($u \geq 0$) and retraction ($u < 0$). For most values of the external variables $\bar{u}_t^E > 0$ and $\bar{u}_t^R < 0$, thus ψ_t is a time-varying 'deadzone' nonlinearity, with the more familiar description

$$\psi_t(u) = \begin{cases} M_t^E(u - \bar{u}_t^E), & u \geq \bar{u}_t^E \\ 0, & \bar{u}_t^R < u < \bar{u}_t^E \\ M_t^R(u - \bar{u}_t^R), & u \leq \bar{u}_t^R. \end{cases} \tag{4}$$

In some cases, it is possible to have $\bar{u}_t^E < 0$ and thus ψ_t becomes a 'preload' nonlinearity in extension. Coefficients $M_t^{E/R}$ are always positive. Some instances of ψ_t are shown in Fig. 3 for selected flight conditions.

Remark 1: A step-like shift of TMC_0 can in fact be considered as an input disturbance which can be counteracted by the inclusion of an integral action in the controller. On the other hand, for the purpose of position control, such an

additional integral term is not needed, since integral action is already present in the loop. This is the main motivation for the observer developed in the next section.

III. Observer design

The aim of this section is to describe the design of a nonlinear observer for the plant described by equations (1)-(2). The observer should reconstruct x_2 using w and x_1. The key technical difficulty with the construction of the observer is that the plant has two poles at the origin and no "gain" for small values of the argument $w - x_2$ of the static input nonlinearity — see (4). This means that it is impossible to distinguish between different values of x_2 when $w - x_2$ lies inside the deadzone of ψ_t. Hence, it is not possible to obtain asymptotic stability of the observation error. In order to overcome this difficulty, we will initially follow the approach of [7], [8] (see also [9]) to design an observer for the plant as if the deadzone was replaced by a more benign nonlinearity, plus a bounded perturbation. Then, we will show that a nonlinear observer, constructed using the more benign nonlinearity, allows us to conclude ultimate boundedness of the observation error, with the ultimate bound depending, quite logically, on the parameters of the 'deadzone' ψ_t. The reason for the modification of the technique [8] is explained in more detail in Appendix A. It is again emphasized that the combination of imaginary axis poles and a lack of gain around the origin, prevent the application of standard design tools and force us to use alternative techniques. If the nonlinearity was slope-restricted and the plant *asymptotically stable*, it would be feasible to use techniques similar to those of [10], [11], [13] in order to prove asymptotic stability of the error system. If the nonlinearity was, instead, 'saturation-like' (non-zero gain near the origin), it would be possible to use techniques similar to, for example, those described in [12], to again prove asymptotic stability. In the case we consider here, the plant is not asymptotically stable and the nonlinearity in question is 'deadzone-like'; different tools are needed.

In order to start with the approach of [7], [8], we rearrange equations (1)-(3) as:

$$\dot{x} = \mathbf{A}x + \mathbf{G}\gamma_t(\mathbf{H}x, w) + \mathbf{G}b_t(\mathbf{H}x, w) \tag{5}$$

$$y = \mathbf{C}x \tag{6}$$

where $x = [x_1\ x_2]'$,

$$\mathbf{A} = \begin{bmatrix} 0 & -1 \\ 0 & 0 \end{bmatrix}, \quad \mathbf{G} = \begin{bmatrix} 1 \\ 0 \end{bmatrix}, \quad \mathbf{H} = \begin{bmatrix} 0 & 1 \end{bmatrix}, \quad \mathbf{C} = \begin{bmatrix} 1 & 0 \end{bmatrix}, \tag{7}$$

and

$$\gamma_t(a, w) = \begin{cases} a + M_t^E(w - a), & w - a \geq 0, \\ a + M_t^R(w - a), & w - a < 0, \end{cases} \tag{8}$$

$$b_t(a, w) = \begin{cases} \psi_t(w - a) - M_t^E(w - a), & w - a \geq 0, \\ \psi_t(w - a) - M_t^R(w - a), & w - a < 0. \end{cases} \tag{9}$$

In (5)-(9) we have rearranged equations in order to obtain the structure considered in [7], [8], but we have also split the original input nonlinearity ψ_t into the two components γ_t (the "benign" nonlinearity), which does not have a deadzone, and b_t which is the more troublesome part.

Let us define

$$M_{\max} = \max\left\{\sup_t M_t^E, \sup_t M_t^R\right\}, \tag{10}$$

$$M_{\min} = \min\left\{\inf_t M_t^E, \inf_t M_t^R\right\}, \tag{11}$$

$$\bar{u}_{\max} = \max\left\{\sup_t |\bar{u}_t^E|, \sup_t |\bar{u}_t^R|\right\}. \tag{12}$$

Then, the following two facts are crucial for establishing our results and are proved in Appendix B.

Fact 1:

$$\|b_t(a, w)\| \leq M_{\max}\bar{u}_{\max} \tag{13}$$

Fact 2:

$$1 - M_{\max} \leq \frac{\gamma_t(a, w) - \gamma_t(b, w)}{a - b} \leq 1 - M_{\min} \tag{14}$$

for any $a, b, a \neq b, w$ and t.

Fact 1 simply establishes a bound on the magnitude of the nonlinearity b_t and will be used to obtain boundedness of the observation error. Fact 2 shows that the nonlinearity γ_t is slope restricted within the interval $[1 - M_{\max}, 1 - M_{\min}]$. In this paper we have

$$M_{\min} \leq M_{\max} < 1 \tag{15}$$

so the slope of γ_t is always positive.

We consider the observer

$$\dot{\hat{x}} = \mathbf{A}\hat{x} + \mathbf{L}(\mathbf{C}\hat{x} - y) + \mathbf{G}\gamma_t(\mathbf{H}\hat{x} + \mathbf{K}(\mathbf{C}\hat{x} - y), w). \tag{16}$$

where $\mathbf{L}$ is a matrix which performs a similar function to a linear observer gain and $\mathbf{K}$ is a scalar used in the nonlinear portion of the observer as proposed in [7]. The corresponding dynamic equation of the error $e = x - \hat{x}$ can be written as

$$\dot{e} = (\mathbf{A} + \mathbf{L}\mathbf{C})e + \mathbf{G}\varphi + \mathbf{G}\delta \tag{17}$$

$$\varphi = \gamma_t(\mathbf{H}x, w) - \gamma_t(\mathbf{H}\hat{x} + \mathbf{K}(\mathbf{C}\hat{x} - y), w) \tag{18}$$

$$\delta = b_t(\mathbf{H}x, w) \tag{19}$$

If we had $\delta = 0$ then the error dynamics would have the structure considered in [7], [8] and an LMI condition for asymptotic stability could be formulated. Here we follow a similar approach but, due to the presence of δ, we can only obtain ultimate boundedness.

Let us assume that there exists a positive definite matrix $\mathbf{P} > 0$, a positive scalar $v > 0$, a matrix $\mathbf{L}$ and a scalar $\mathbf{K}$ such that

$$\begin{bmatrix} (\mathbf{A} + \mathbf{L}\mathbf{C})'\mathbf{P} + \mathbf{P}(\mathbf{A} + \mathbf{L}\mathbf{C}) + v\mathbf{I} & \mathbf{P}\mathbf{G} + (\mathbf{H} + \mathbf{K}\mathbf{C})' \\ \mathbf{G}'\mathbf{P} + (\mathbf{H} + \mathbf{K}\mathbf{C}) & -\dfrac{2}{1 - M_{\min}} \end{bmatrix} \leq 0\,. \tag{20}$$

Remark 2: Condition (20) is an LMI in $\mathbf{P}$, $\mathbf{PL}$, v and $\mathbf{K}$.

Remark 3: Observability of $(\mathbf{C}, \mathbf{A})$, always implies the existence of a matrix $\mathbf{L}$ for any scalar $v > 0$ such that the

(1,1) entry of LMI (20) is negative definite. Furthermore, the (2,2) entry is also negative definite in view of $M_{\min} < 1$.

Consider the Lyapunov function $V(e) = e'\mathbf{P}e$. Then, we have

$$\dot{V}(e) = \begin{bmatrix} e \\ \varphi \end{bmatrix}' \begin{bmatrix} (\mathbf{A}+\mathbf{LC})'\mathbf{P} + \mathbf{P}(\mathbf{A}+\mathbf{LC}) & \mathbf{PG} \\ \mathbf{G}'\mathbf{P} & 0 \end{bmatrix} \begin{bmatrix} e \\ \varphi \end{bmatrix} + \\ + 2e'\mathbf{PG}\delta \quad (21)$$

$$\leq \begin{bmatrix} e \\ \varphi \end{bmatrix}' \begin{bmatrix} -v\mathbf{I} & -(\mathbf{H}+\mathbf{KC})' \\ -(\mathbf{H}+\mathbf{KC}) & \frac{2}{1-M_{\min}} \end{bmatrix} \begin{bmatrix} e \\ \varphi \end{bmatrix} + 2e'\mathbf{PG}\delta \quad (22)$$

$$= -ve'\mathbf{I}e - 2\varphi(\mathbf{H}+\mathbf{KC})e + \frac{2}{1-M_{\min}}\varphi^2 + 2e'\mathbf{PG}\delta \quad (23)$$

$$\leq -ve'\mathbf{I}e + 2e'\mathbf{PG}\delta. \quad (24)$$

in which we have used

$$\varphi(\mathbf{H}+\mathbf{KC})e \geq \frac{1}{1-M_{\min}}\varphi^2\,. \quad (25)$$

This inequality follows because from Fact 2, we have that

$$(1-M_{\max})(a-b) \leq \gamma_t(a,w) - \gamma_t(b,w) \\ \leq (1-M_{min})(a-b) \quad (26)$$

Thus, using (18), it follows that

$$(1-M_{\max})(\mathbf{H}+\mathbf{KC})e \leq \varphi \leq (1-M_{min})(\mathbf{H}+\mathbf{KC})e \quad (27)$$

which implies we can write

$$\varphi = \theta_t(\mathbf{H}+\mathbf{KC})e \quad (28)$$

where $\theta_t \in [1-M_{\max}, 1-M_{min}]$. Hence inequality (25) can be re-written as

$$\frac{\theta_t}{1-M_{\min}}(1-M_{\min}-\theta_t)\|(\mathbf{H}+\mathbf{KC})e\|^2 \geq 0 \quad (29)$$

and, noting (15), it follows that this is true for all $\theta_t \in [1-M_{\max}, 1-M_{min}]$.

Note that, if we had $\delta = 0$ then (24) would imply asymptotic stability of the observation error. Instead, taking into account δ we can write

$$\dot{V}(e) \leq -v\|e\|^2 + 2\|e'\|\|\mathbf{PG}\|\|\delta\| \quad (30)$$

From Fact 1 it then follows that $\|\delta\| \leq M_{\max}\bar{u}_{\max}$. Hence, we obtain

$$\dot{V}(e) \leq -\|e\|(v\|e\| - 2\|\mathbf{PG}\|M_{\max}\bar{u}_{\max}). \quad (31)$$

From (31) it then follows that $e(t)$ converges to the smallest sub-level set of $V(e)$ containing the set

$$\{e : \|e\| \leq (2/v)\|\mathbf{PG}\|M_{\max}\bar{u}_{\max}\}\,. \quad (32)$$

or, in other words, the error state is globally uniformly ultimately bounded [14].

Remark 4: Note that the structure of the observer given in equation (16) does not require an *exact duplicate* of the nonlinearity ψ_t: it simply requires the portion of ψ_t replicated in γ_t to be known. This means that the observer requires knowledge of the "gain" variation $M_t^{E/R}$ but *not* knowledge of the dead-band $\bar{u}_t^{E/R}$, although - not surprisingly - the ultimate bound depends on the width of this dead-band as indicated in equation (32).

IV. Simulations

In this section, we present some simulation examples generated using the Trent 1000 RSS. The Trent 1000 RSS is a large Simulink model which, among other components, includes the HMU and the VSV Actuator depicted in Fig. 1. In the RRS, the actuation system is implemented by a full nonlinear hydro-mechanical model. In this work, the observer has been designed on the basis of the simplified model described in Section II but is illustrated using the full nonlinear simulator. The simulations presented in this section are generated using the VSVA component in closed-loop with its controller. The operating point is representative of a 'ground idle' state. The numerical values of the corresponding parameters are: $M^E = 2.74\text{mm}\,\text{s}^{-1}\,\text{mA}^{-1}$, $M^R = 0.24\text{mm}\,\text{s}^{-1}\,\text{mA}^{-1}$, $\bar{u}^E = 0.0484\text{mA}$, $\bar{u}^R = -1.4519\text{mA}$. The simulations were generated using sinusoidal reference signals within the bandwidth of the VSVA closed-loop system (1.6Hz).

In this section, we illustrate the performance of the observer developed in Section III, and of a variant based on full knowledge of the plant, i.e. in which γ_t in (8) includes an exact duplicate of ψ_t including the deadzone. Note that, due to the characteristics of the deadzone, even for this version of the observer it is not possible to obtain asymptotic stability of the observation error. Indeed, it can be shown that the analysis of Section III applies with minimal modifications and leads to similar conclusions. However, this modified version of the observer makes use of exact knowledge of the plant and in some simulations appears to have better performance. In both cases the observer parameters were

$$\mathbf{L} = [-1.7145 \quad 0.7634]', \quad \mathbf{K} = -1.8113$$

and

$$v = 0.0064, \quad \mathbf{P} = \begin{bmatrix} 3.1807 & 1.0126 \\ 1.0126 & 4.6470 \end{bmatrix}$$

obtained by a simple search for a feasible solution of the LMI (20). The resulting bound on the right-hand side of the inequality of section is 170mA (thus not useful in practice).

In Fig. 4 and Fig. 5 respectively, the control input (TMC) and the actuator's position (x_1) of the first simulation experiment are displayed. In Fig. 4 the limits of the input deadzone are also displayed. Note that the deadzone is smaller on the positive side (compare with Fig. 3). In this simulation experiment, the value of TMC_0 (x_2) was initially set at 12mA and was subject to a step-like shift to 16mA at time 800s. The observer was initialised at the nominal value $TMC_0 = 14.6\text{mA}$. In Fig. 6 we illustrate the performance of the two versions of the observers. In the figure, the value

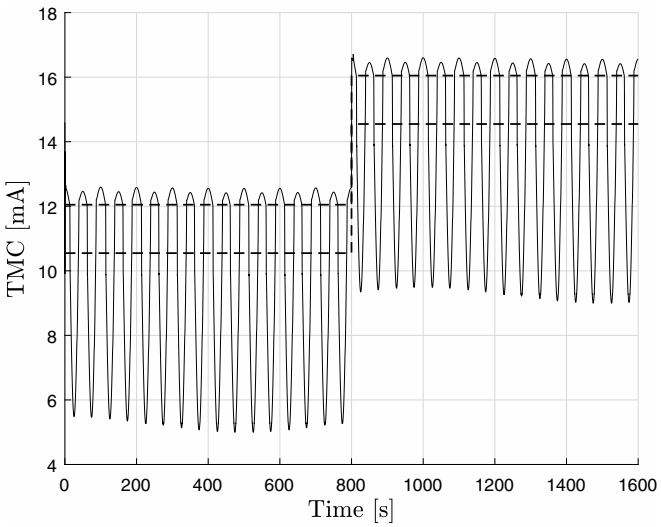

Fig. 4. Input TMC (solid thin) and limits of the deadzone (dash bold).

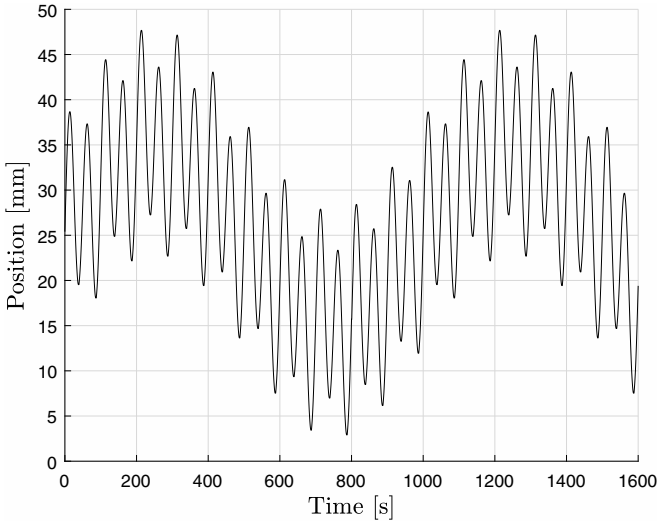

Fig. 5. Position of the actuator.

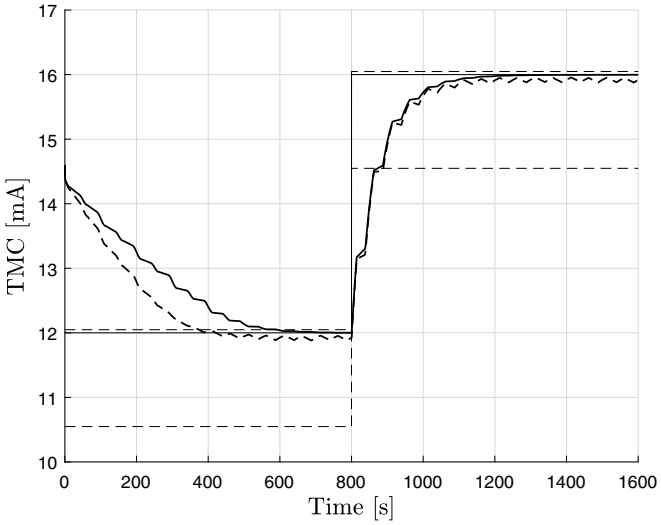

Fig. 6. True TMC_0 (solid thin), limits of the deadzone (dash thin), and estimated TMC_0: observer with full knowledge of ψ_t (solid bold) observer with partial knowledge of ψ_t (dash bold).

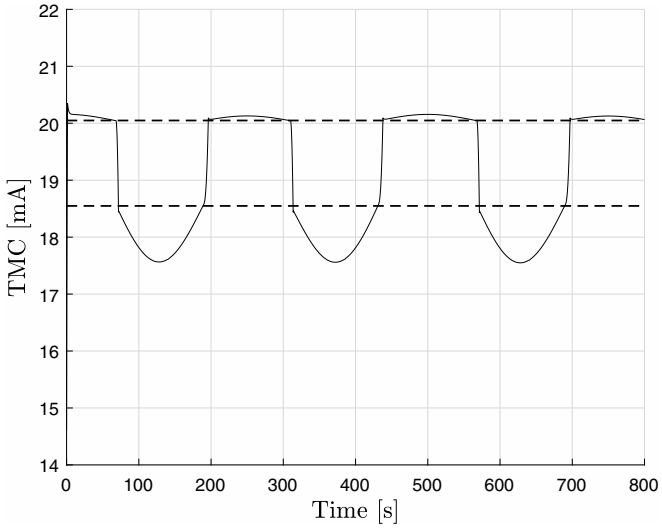

Fig. 7. Input TMC (solid thin) and limits of the deadzone (dash bold).

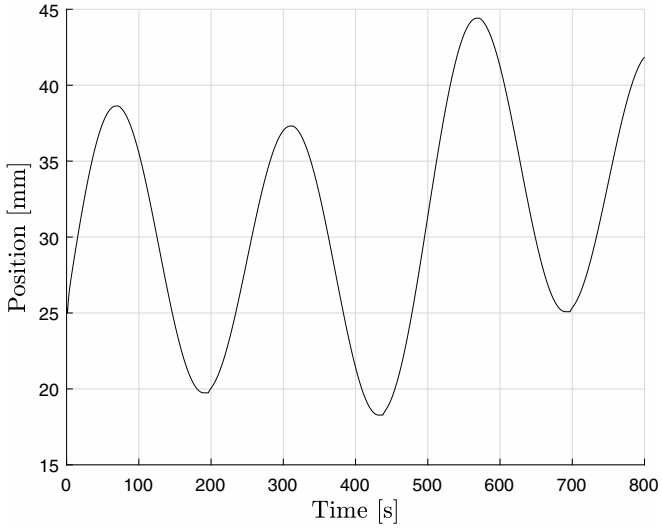

Fig. 8. Position of the actuator.

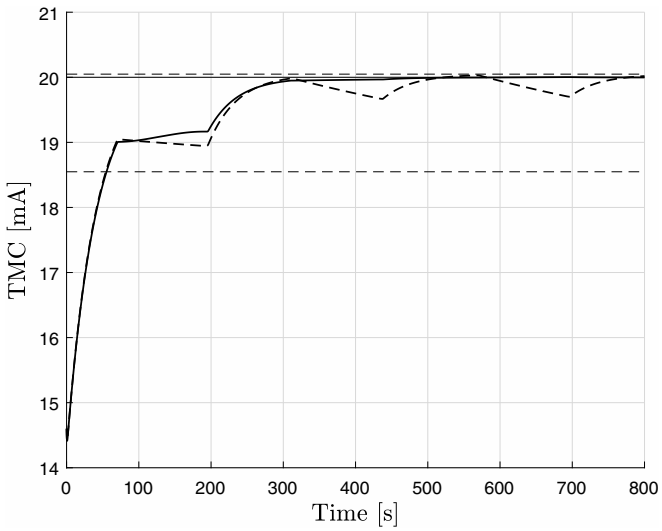

Fig. 9. True TMC_0 (solid thin), limits of the deadzone (dash thin), and estimated TMC_0: observer with full knowledge of ψ_t (solid bold) observer with partial knowledge of ψ_t (dash bold).

of TMC_0 is displayed together with the deadzone region around it. In Fig. 6 it can be seen that both estimated states converge towards the true TMC_0 as expected. In the case of the observer with full knowledge of ψ_t, the estimated TMC_0 appears to converge to the true TMC_0.

In the second simulation experiment, the value of TMC_0 (x_2) was set at $20\mathrm{mA}$ and the observer was again initialised at the nominal value $TMC_0 = 14.6\mathrm{mA}$. The results are illustrated in Fig.s 7-9. In this simulation experiment, similarly to the previous case, both estimated states converge to or near the actual state despite the deadzone, but the difference in behaviour of the two observers is more noticeable.

V. Conclusion

We have formulated the design of a nonlinear observer motivated by the problem of detecting null-current shifts in an electro-hydraulic actuation system. The following open issues are the object of current investigation.

The observer assumes perfect knowledge of the coefficients M_t^E and M_t^R, but not of $\bar{u}_t^E$ and $\bar{u}_t^R$. In turn, the coefficients of ψ_t depend on the engine's speed and on the aerodynamic load. Although the engine speed can be considered known with sufficient accuracy, the aerodynamic load can be subject to considerable variations with respect to its nominal values. Hence, an analysis of the observer's properties without perfect knowledge of any of these coefficients is desirable. Although in the simulation section it has been shown that an observer with an exact replica of ψ_t appears to converge to the true TMC_0 in some examples, in general it is not possible to obtain asymptotic stability of the observation error even with perfect knowledge of ψ_t. In the simulation section it has also been shown that the estimated state converges near to the actual state without perfect knowledge of ψ_t. In practice, this feature could be enough for detecting a fault.

Finally, the design variables $\mathbf{L}$ and $\mathbf{K}$ were obtained by the solution of the feasibility problem for the LMI condition (20). Instead, it would desirable to have a design criterion for choosing $\mathbf{L}$ and $\mathbf{K}$, possibly taking into account the guaranteed bounds (32).

APPENDIX

A. Motivation for Modification

At first glance, the problem considered in this paper looks similar to that considered in [8], where the plant is assumed to have the form:

$$\dot{x} = \tilde{\mathbf{A}}x + \tilde{\mathbf{G}}\psi_t(\mathbf{H}x, w) + \rho(y, w) \tag{33}$$

$$y = \mathbf{C}x \tag{34}$$

However, equations (1)-(2) imply $\tilde{\mathbf{A}} = 0_{2\times 2}$ and also it follows that $\mathbf{C} = [1 \quad 0]$, meaning that the pair $(\mathbf{C}, \tilde{\mathbf{A}})$ is not detectable. Although ψ_t is itself slope-restricted, this lack of detectability means that *there do not exist* solutions to the LMI's provided in [8]. The partitioning of the nonlinearity overcomes this problem, by ensuring that the pair $(\mathbf{C}, \mathbf{A})$ is detectable (see expression for $\mathbf{A}$ in main text of paper). In turn, this then raises the possibility that LMI (20) is feasible.

B. Useful Facts

Proof of Fact 1: If $w - a \geq 0$ and $w - a > \bar{u}_t^E$, then, from the definition of $b_t(w, a)$, it follows that $b_t(w, a) = -M_t^E \bar{u}_t^E \Rightarrow |b_t(w, a)| \leq M_{\max}\bar{u}_{\max}$. If $w - a \geq 0$ and $w - a \leq \bar{u}_t^E$, then $b_t(w, a) = M_t^E(w - a) \leq M_{\max}\bar{u}_{\max}$. Corresponding inequalities are obtained when $w - a < 0$.

Proof of Fact 2: Let $\varphi_t(a, b, w) = \gamma_t(a, w) - \gamma_t(b, w)$. If $w - a \geq 0$ and $w - b \geq 0$ we have $\varphi_t(a, b, w) = (1 - M^E)(a - b)$. Similarly, if $w - a < 0$ and $w - b < 0$ we have $\varphi_t(a, b, w) = (1 - M^R)(a - b)$. If $w - a \geq 0$ and $w - b < 0$, and thus $a - b < 0$, we have $\varphi_t(a, b, w) \leq (a-b)+M_{\max}(w-a)-M_{\max}(w-b) = (1-M_{\max})(a-b)$, and, similarly, $\varphi_t(a, b, w) \geq (1 - M_{\min})(a - b)$. Analogous inequalities are obtained when $w - a \geq 0$ and $w - b < 0$.

References

[1] T. Puller, A. Lecchini-Visintini, A simplified model of a fueldraulic actuator with application to load estimation, submitted, 2017.

[2] T. Puller, A. Lecchini-Visintini, Modelling for control of a jet engine compressor variable stator vanes hydraulic actuator. European Control Conference, Aalborg, 2016.

[3] Instrument Engineers' Handbook, Volume 3: Process Software and Digital Networks, Fourth Edition, B.G. Liptak, H. Eren, editors, CRC Press, 2016.

[4] G. P. Liu, S. Daley, Optimal-tuning nonlinear PID control of hydraulic systems, Control Engineering Practice, 8(9):1045-1053, 2000.

[5] I.-Y. Lee, D.-H. Oh, , S.-W. Ji, , S.-N. Yun, Control of an overlap-type proportional directional control valve using input shaping filter, Mechatronics, 29:8795, 2015.

[6] M. Jelali, A. Kroll, Hydraulic Servo-systems, Modelling, Identification and Control. Springer-Verlag, 2004.

[7] M. Arcak, P. Kokotović, Nonlinear observers: a circle criterion design and robustness analysis, Automatica, 37(12), 2001.

[8] M. Arcak, P. Kokotović, Observer-based control of systems with slope-restricted nonlinearities, IEEE Trans. Automatic Control, 46(7), 2001.

[9] A.Lj. Juloski, W.P.M.H. Heemels, S. Weiland, Observer design for a class of piecewise linear systems, Int. J. Robust Nonlinear Control, 17(15), 2007.

[10] P.G. Park. Stability criteria of sector and slope restricted Lur'e systems. *IEEE Trans. Aut. Control*, 47(2):308–313, 2002.

[11] M.C. Turner and M. Kerr. Lyapunov functions and $\mathcal{L}_2$-gain bounds for systems with slope restricted nonlinearities. *Systems & Control Letters*, 69:1–6, 2014.

[12] F. Tyan, D. S. Bernstein. Global stabilization of systems containing a double integrator using a saturated linear controller. *Int. J. Rob. and Nonlinear Contr.*, vol. 9, no. 15, pp. 1143–1156, 1999.

[13] G. Valmorbida, R. Drummond, and S.R. Duncan. Positivity conditions of Lyapunov functions for systems with slope restricted nonlinearities. In *American Control Conference*, pages 258–263, 2016.

[14] H.K. Khalil. *Nonlinear Systems*. Prentice Hall, New Jersey, 1996.

[15] Carrasco, J., Turner, M.C., and Heath, W.P. (2016). Zames–Falb multipliers for absolute stability: From O' Shea's contribution to convex searches. *European Journal of Control*, 28, 1–19.

[16] Leonov, G., Ponomarenko, D., and Smirnova, V. (1996). *Frequency-Domain Methods for Nonlinear Analysis*. World Scientific, Singapore.

[17] C. A. Desoer and M. Vidyasagar. *Feedback Systems: Input-Output Properties*. Academic Press, Inc., Orlando, FL, USA, 1975.

[18] H. J. Marquez. *Nonlinear Control Systems: Analysis and Design*. John Wiley and Sons, Hoboken, NJ, USA, 2003.